

NASA Contractor Report 194454

1N-20  
206656  
22P

# Stationary Plasma Thruster Plume Characteristics

Roger M. Myers and David H. Manzella  
*Sverdrup Technology, Inc.*  
*Lewis Research Center Group*  
*Brook Park, Ohio*

Prepared for  
Lewis Research Center  
Under Contract NAS3-25266

**NASA**  
National Aeronautics and  
Space Administration

N94-24361

unclas

0206656

G3/20

(NASA-CR-194454) STATIONARY PLASMA  
THRUSTER PLUME CHARACTERISTICS  
Final Report (Sverdrup Technology)  
22 p

1

2

3

4

5

6

7

8

# STATIONARY PLASMA THRUSTER PLUME CHARACTERISTICS

Roger M. Myers<sup>1</sup> and David H. Manzella<sup>2</sup>  
Sverdrup Technology, Inc.  
NASA Lewis Research Center Group  
Brookpark, OH 44142

## Abstract

Stationary Plasma Thrusters (SPTs) are being investigated for application to a variety of near-term missions. This paper presents the results of a preliminary study of the thruster plume characteristics which are needed to assess spacecraft integration requirements. Langmuir probes, planar probes, Faraday cups, and a retarding potential analyzer were used to measure plume properties. For the design operating voltage of 300 V the centerline electron density was found to decrease from  $\sim 1.8 \times 10^{17} \text{ m}^{-3}$  at a distance of 0.3 m to  $1.8 \times 10^{14} \text{ m}^{-3}$  at a distance of 4 m from the thruster. The electron temperature over the same region was between 1.7 and 3.5 eV. Ion current density measurements showed that the plume was sharply peaked, dropping by a factor of 2.6 within 22 degrees of centerline. The ion energy 4 m from the thruster and  $15^\circ$  off-centerline was  $\sim 270 \text{ V}$ . The thruster cathode flow rate and facility pressure were found to strongly affect the plume properties. In addition to the plume measurements the data from the various probe types were used to assess the impact of probe design criteria.

## Nomenclature

$A_p$	probe surface area, $\text{m}^2$
$e$	electron charge, $1.6 \times 10^{-19} \text{ C}$
$E$	particle energy, J
$f_i(E)$	ion energy distribution function
$I_e$	electron current, A
$I_{e,s}$	electron saturation current, A
$j_i$	ion current density, $\text{A/m}^2$
$j_{i,v}$	ion current under perfect vacuum, $\text{A/m}^2$
$k$	Boltzmann's constant, $1.38 \times 10^{-23} \text{ J/K}$
$m_e$	electron mass, $9.11 \times 10^{-31} \text{ kg}$
$n_e$	electron number density, $\text{m}^{-3}$
$n_i$	ion number density, $\text{m}^{-3}$
$r_p$	probe radius, m
$T_e$	electron temperature, K
$v_i$	ion velocity, m/s
$V_p$	probe bias voltage, V
$z$	distance from thruster, m
$Z$	ion charge
$\lambda_{ce}$	charge exchange mean free path, m
$\lambda_d$	Debye length, m
$\phi$	grid potential, V

## Introduction

Stationary Plasma Thrusters (SPTs) have been flown on over 50 Russian spacecraft and are currently being considered for application to stationkeeping, repositioning, and orbit transfer missions in the United States.<sup>1-6</sup> An SPT, shown schematically in Fig. 1, consists of an annular chamber with insulating walls within which an electric discharge is sustained between an external hollow cathode and a ring shaped anode at the rear of the chamber. Electromagnets are used to generate a radial magnetic field within the chamber which reduces the electron conductivity and permits the plasma to sustain a large axial electric field. The xenon propellant ions are accelerated axially by the electric field. Xenon propellant is used because of its low ionization potential and high molecular weight. While the details of the acceleration mechanism are not fully understood, the thruster has been perfected in Russia to the point where its performance appears to exceed that of competing technologies for some applications.<sup>7,8</sup>

This work was part of an effort to characterize the performance, PPU interfaces, and spacecraft integration issues associated with the operational use of SPTs for stationkeeping and primary propulsion applications.

<sup>1</sup>Propulsion Engineer, member AIAA

<sup>2</sup>Propulsion Engineer

Papers by Sankovic, et al.,<sup>9</sup> Hamley, et al.,<sup>10</sup> Pencil,<sup>11</sup> and Manzella<sup>12</sup> discuss the performance, PPU, contamination, and optical characteristics of the thruster tested at NASA LeRC. This paper focusses on measurements of the SPT plume properties in an attempt to establish a data base from which plume/spacecraft interactions can be assessed.

The integration of electric thrusters onto spacecraft has been extensively studied for ion thrusters and arcjets.<sup>13-17</sup> Integration issues include momentum and thermal loading of spacecraft surfaces, erosion and contamination of those surfaces, electromagnetic noise generation, and interference with up and downlink communication signals. The exhaust of the SPT thruster is known to be highly ionized with a mass average velocity of between 14000 m/s and 18000 m/s.<sup>2</sup> The high energy exhaust can sputter surfaces with which it interacts causing concern not only about erosion of spacecraft surfaces, but also about contamination of surfaces by eroded thruster material. The highly ionized plume may interfere with communications signals by refracting the electromagnetic waves as they propagate through the variable density expanding plasma.<sup>15</sup> Some of these issues were recently investigated by Absalamov, et al.<sup>18</sup> who used planar and gridded ion probes and solar cell cover glass samples to establish the potential impact of the thruster on the spacecraft. That work was done in a 2.5 m diameter by 6 m long cryopumped facility which maintained a pressure near  $6.7 \times 10^{-3}$  Pa during thruster operation. Under these conditions the vacuum chamber size and pressure could have influenced the measurements,<sup>19</sup> making it important to test the thruster in a larger facility with higher pumping speed.

This paper presents preliminary results of an effort to establish appropriate probe geometries and plume characteristics of an SPT-100 thruster. Following a description of the experimental facility and probes, measurements of the plume characteristics at distances of 0.3 m, 2 m, and 4 m from the thruster are presented. Langmuir probes, Faraday cups, planar probes, and a retarding potential analyzer (RPA) were used to establish the electron density, electron temperature, ion current density, and ion energy at several angles from the thruster axis. In addition, the results from the various probe types are compared to establish criteria for improved probe designs. Finally, a summary of the study conclusions is presented.

## Experimental Apparatus

### Thruster and Support Equipment

The SPT-100 thruster used in this study was provided by the Ballistic Missile Defense Organization (BMDO) and was constructed at Fakel Enterprises in Kaliningrad (Baltic Region), Russia. The thruster was used without modification. The power processing unit used for these tests was built by Hamley, et al.<sup>10</sup> The original thruster flow control system was bypassed by connecting xenon feed lines directly to the thrust chamber and cathode supply lines. This provided the ability to independently vary the chamber and cathode flow rates.<sup>9</sup> Calibration techniques and results are discussed in detail by Sankovic, et al.<sup>9</sup> and Hamley, et al.<sup>10</sup>

### Facility

The tests were conducted using the NASA LeRC Tank 5 vacuum facility, which is 4.6 m in diameter and 18 m long, with a 41 m<sup>2</sup>, 20 K gaseous helium cryopump. For the near-field plume measurements the thruster was mounted on a thrust stand located on the centerline of a 1 m diameter, 1 m long spool-piece mounted on the side of the main tank. As shown in Figure 2, the thruster exit plane was approximately 1 m from the main tank during these tests. Ambient pressure was measured using an ion gauge calibrated for air which was located on the spool-piece. The ion gauge readings were corrected for xenon by dividing by 3.1. The normal ambient pressure during thruster operation was  $1.7 \times 10^{-3}$  Pa, though this was varied during testing by bleeding in gas from an external source. For the far-field plume measurements, the thruster was located in the main tank as shown in Fig. 3, and fired toward the helium cryopump. The ambient pressure at the thruster was normally  $6.7 \times 10^{-4}$  Pa for these tests, though it was varied in the same manner as was done with the near-field measurements.

### Near-Field Plume Diagnostics

A cylindrical Langmuir probe was used to characterize the near-field SPT plume. These measurements were made simultaneously with the performance measurements described by Sankovic.<sup>9</sup> As shown in Fig. 2, the probe was mounted on a cantilevered arm which could be rotated around the thruster centerline at a constant distance of 31 cm from the centerline of thruster exit plane. The probe always pointed at the thruster centerline. The probe was a 1.57 cm long, 0.051 cm diameter piece of tungsten wire

extending from a 1 mm outer diameter, 5 cm long alumina insulator.

The probe was biased relative to the tank wall using the circuit shown in Figure 4. The function generator drove the bipolar amplifier using a 1 kHz triangle wave. The audio transformer between the function generator and the amplifier served to isolate the probe circuit from the function generator ground. The probe current was measured using a 10-ohm shunt, and the probe voltage with respect to ground was measured directly. The probe voltage and current waveforms were recorded on a digital oscilloscope at a rate of 1 MHz. Between twelve and sixteen complete probe voltage-current (V-I) characteristics were obtained at each location and operating condition. The final results are the average values for all the V-I characteristics collected at a given location and operating condition, and error bars reflect the corresponding standard deviations.

All of the near-field Langmuir probe data were reduced using standard thin-sheath probe theory.<sup>20</sup> The validity of this theory for the plasma conditions found in the plume will be discussed below. In this analysis, the electron temperature is obtained from:

$$T_e = \frac{e}{k} \left( \frac{d(\ln(I_e))}{dV_p} \right)^{-1} \quad (1)$$

where the electron current is obtained by subtracting the ion saturation current from the entire current trace. The electron density is obtained from:

$$n_e = \frac{I_{e,s}}{eA_p} \sqrt{\frac{2\pi m_e}{kT_e}} \quad (2)$$

where  $I_{e,s}$ , electron saturation current, is the current level at the intersection of the linear curve fits to the electron retarding region and the electron saturation region. The corresponding voltage is the local plasma potential. While the data reduction was highly automated, considerable user input was required to ensure that the proper regions were used in the curve-fitting. This was complicated by the wide range of plasma conditions studied in this work, and by the occasional appearance of noise on the probe traces. The probe V - I characteristics were examined individually to ensure proper data reduction.

## Far-Field Plume Diagnostics

### Probe Locations

The far-field probes were arranged in two arcs at radii of 2 m and 4 m from the thruster exit plane. These distances were chosen in an attempt to establish the impact of facility effects on the plume expansion. The probe layout is shown schematically in Figure 3, and Table I lists the probes at each location. Multiple probes were placed at several of the locations so that data from different probe types could be compared. The thruster was fired toward the helium cryopump, with the probes between the thruster and the pump. The support structures, shown in the photograph in Figure 5, consisted of a 1.3 cm diameter stainless steel tube with 0.635 cm diameter, 40 cm long stainless steel vertical supports. The probes extended a minimum of 10 cm in front of the vertical supports.

### Langmuir probes

Stainless steel spherical probes 0.95 cm in radius were used to establish the far-field electron density and temperature. The probe size was selected to obtain a minimum probe radius to Debye length ratio of 10 by extrapolating published electron density results for the thruster exit plane according to a  $1/r^2$  dependence.<sup>2</sup> Spherical probes were selected for this first test series because of their relatively well-known behavior across a wide variety of plasma densities and their lack of sensitivity to the plasma velocity vector.

Each probe was supported using a 20 cm length of 0.79 cm diameter aluminum oxide tubing mounted to a vertical piece of 0.635 cm diameter stainless steel rod using a clamp. The probe conductor was placed inside the aluminum oxide support which extended from the probe away from the thruster. The arrangement yielded a net exposed probe area of 10.9 cm<sup>2</sup>, though the actual current collecting area might be reduced by the formation of a probe wake.<sup>21</sup> Because the alumina support rod was behind the probe and covered 10% of the original probe surface, the maximum reduction in exposed probe area which could result from a probe wake was 40%.

The probes were cleaned with acetone and ethyl alcohol immediately before closing the tank. The probes were biased using the same circuit as for the near-field plume measurements (Fig. 4) and the data were reduced in the same fashion.

### Planar Probes & Faraday Cups

Two types of ion current probes, shown in Figure 6, were evaluated. The first was a simple planar probe, consisting of a 5.1 cm diameter molybdenum disk facing the thruster. All planar probes were built with grounded guard rings. The guard ring consisted of a 3.81 cm inner diameter, 0.635 cm wide molybdenum ring supported 0.3 cm above the planar probe. The second probe was a Faraday cup. The Faraday cup walls, which were biased to the same potential as the collector, were meant to repel secondary electrons emitted by the collector and prevent an erroneously high current reading. Faraday cups were tested with and without guard rings to establish the guard ring effect on probe response. For these tests the base of the Faraday cup was molybdenum, and the cup wall and entry lip were stainless steel. The cup aperture was the same diameter as the opening in the planar probe guard rings, and the cup depth was twice the aperture diameter. The side wall diameter was 5.1 cm, and the probe was carefully aligned with the thruster to preclude direct impingement of plume ions on the side of the cup. The entire outer surface of the cups were insulated using dielectric tape. The entire probe was electrically common, so that when biased negative the walls of the probe repelled secondary electrons emitted from the base collector. All of the ion current probes had aperture areas of 11.4 cm<sup>2</sup>.

The ion current probes were biased relative to the tank wall using a 100 V power supply. A 100 ohm shunt, connected between the power supply and the tank wall, was used to measure the probe current.

### Retarding Potential Analyzer

A retarding potential analyzer (RPA), which measures ion flux as a function of ion energy, was used to assess ion energies at a distance of 4 m from the SPT exit plane at a 15° angle from center line. The probe design was based on a flight-qualified RPA developed during the Ion Auxiliary Propulsion System (IAPS) flight program<sup>22</sup> and consisted of four equally spaced tungsten grids and a molybdenum ion collector. The outermost grid and attached guard ring were maintained at facility ground to minimize the perturbing effect on the SPT plume. The second grid repelled incoming electrons. It was biased at a constant voltage between -10 V and -30 V. The third grid was used as a variable voltage ion suppressor transmitting only those ions with kinetic energies greater than  $eZ\phi$ , where  $e$  is the electronic charge,  $Z$  is the charge of the ion (1 for a

singly charged ion) and,  $\phi$  is the ion suppressor grid potential. The inner grid was biased to the same voltage as the second grid. This grid repelled secondary electrons emitted from the collector. The aperture for the probe was 38 mm in diameter. The grids were constructed from 0.13 mm diameter tungsten wires spaced 4 mm apart. The open area fraction for each grid was estimated to be 0.87. For this test no attempt was made to calibrate the overall grid transmittance. A schematic of the probe is shown in Figure 7.

The circuit used to drive the RPA is shown in Figure 8. The current through the molybdenum collector was measured with a digital storage oscilloscope as the voltage drop across a calibrated load resistor. A programmable function generator was used to drive the high voltage ion suppressor bias supply at a frequency of 0.15 Hz. This voltage was recorded by the digital storage oscilloscope. All voltages were measured relative to the facility ground. The voltage to the electron repeller was preset and the ion suppressor voltage was driven with a 700 V sawtooth. The current and the ion suppressor voltage were simultaneously recorded on the oscilloscope and subsequently transferred to a personal computer. Data reduction included smoothing of the data and calculating the first derivative of the ion current as a function of retarding potential, which yields the ion distribution function:

$$f_i(E) = -\frac{dj_i}{d\phi} \frac{1}{e} \sqrt{\frac{m_i}{2e\phi}} \quad (3)$$

## Results

### Behavior of Diagnostics

The first step in this study was to establish the impact of probe contamination, the use of guard rings, and the ion probe type on the plume measurements. The effect of probe surface contamination was assessed prior to the collection of plume data. This was done by looking for hysteresis in the Langmuir probe trace and by examining the reproducibility of Langmuir probe and ion current probe measurements after biasing them to ~ -80 V for 5 minutes while they were in the thruster plume. Hysteresis in the Langmuir probe current has been correlated with surface contaminants,<sup>23,24</sup> and biasing probes sufficiently negative for ion sputtering

to clean their surfaces is a standard cleaning technique.<sup>25</sup> The results of these efforts showed that while contamination was certainly present on all probes at the start of an SPT test it could be easily removed, and in fact in most cases could be eliminated by simply waiting for the high energy thruster plume to clean the surface without resorting to negative biasing.

Figure 9 shows the probe current density measured as a function of probe bias voltage for the two ion current probes located 2 m from the thruster at an angle of 52.5° off-axis. The Faraday probe in this example did not have a guard ring, and it is evident that it collected up to 23% more current than did the planar probe at the same location. If the Faraday probe had been operating properly, the planar probe current density would have been higher than that of the Faraday probe. It appears that because the Faraday probe wall was common with the collector the probe had a larger effective area than the planar probe, even though the aperture size for the two probes was the same. A further example of this effect is shown in Figure 10, which shows similar data for a simple Faraday cup, a Faraday cup with a grounded guard ring, and a planar probe. These probes were in a cluster 2 m from the thruster at an angle of 37.5° off-axis. In this case the simple Faraday cup collected up to twice the ion current density measured by the planar probe, and the current density from the Faraday probe with the guard ring was within 25% of that obtained using the planar probe. The saturation behavior of the Faraday cups indicates that the probe sheath was growing more rapidly with increasing bias voltage than that of the planar probe.<sup>25</sup> This likely occurred because the Faraday cup collector and sides were electrically common. Note that at a bias voltage of -10 V the three probes collect almost the same current and begin to diverge significantly as the bias voltage is decreased. The beneficial effect of the guard ring is evident from the slower rates of ion current rise for the probes using guard rings.

## Plume Characteristics

### Electron Density and Temperature

Electron density and temperature profiles taken at 0.31 m from the thruster at the design point operating conditions of 4.5 A and 300 V are shown in Figures 11 and 12. The results in Figure 11 show the effect of cathode propellant flow rate on the near-field plume characteristics at total flow rates of 5.6 mg/s and 5.4

mg/s. The cathode flow fraction was changed from 5 % to 9 %. Error bars are not visible on the density data because the fluctuations between probe V-I characteristics were too small to appear on the logarithmic scale of the plot. As shown in Figures 11 the centerline density increased from  $\sim 6 \times 10^{16} \text{ m}^{-3}$  to  $1.8 \times 10^{17} \text{ m}^{-3}$  when the cathode flow was increased, and the electron temperature dropped from approximately 3.8 eV to 2 eV. The density profile was sharply peaked, dropping by a factor of three within 22° of the centerline. The electron temperature did not vary significantly with angle, but was markedly different for the two operating conditions. In addition to these quantitative changes, the plume became more quiescent at the higher cathode flow, a result reflected in the smaller error bars on the temperature results. The lack of spatially resolved velocity measurements precludes estimates of mass fluxes from the measured density distributions.

Figures 12 shows electron density and temperature measurements at 2 m and 4 m from the thruster at various angles off-centerline. These measurements were performed simultaneously with the plume contamination and sputtering assessment reported by Pencil.<sup>11</sup> The time integrated nature of those measurements precluded variation of the thruster operating condition and tank pressure except for a single case in which the tank pressure was increased from  $6.7 \times 10^{-4} \text{ Pa}$  to  $4 \times 10^{-3} \text{ Pa}$  by bleeding in nitrogen. For these tests the thruster was operated at total flow rates of 5.31 mg/s and 5.06 mg/s with cathode flow fractions of 5% and 4.2%, respectively. The discharge current was 4.5 A for both cases. The highest measured density at 2 m and  $6.7 \times 10^{-4} \text{ Pa}$  was  $6 \times 10^{14} \text{ m}^{-3}$  at an angle of 7.5° off-centerline. The centerline density dropped to  $1.8 \times 10^{14} \text{ m}^{-3}$  at 4 m from the thruster. When the pressure was increased to  $4 \times 10^{-3} \text{ Pa}$  the density 7.5° off-centerline appeared to increase to  $\sim 8.5 \times 10^{14} \text{ m}^{-3}$ , though the results for the two pressures are within the error bars. The behavior was different off-axis, with only a very small increase in electron density observed at 52.5° and a slight decrease at 67.5°. These results indicate that increasing the facility pressure with nitrogen makes the plume properties more sharply peaked. The electron temperature results in Figure 12b show that for the lowest facility pressure the temperature at 2 m and 4 m from the thruster was essentially constant at 2.2 eV. The lack of angular dependence is similar to the behavior observed at 0.3 m from the thruster, and the results indicate that the

temperature does not decrease rapidly for distances beyond 0.3 m from the thruster. When the tank pressure was increased the temperature increased by approximately 0.6 eV to 2.8 eV.

The effect of thruster operating condition on the plume characteristics 0.3 m from the thruster was also examined at lower discharge voltages. Figures 13a and b show data obtained at thruster voltages of 200 V and 250 V, discharge currents of 4.1 A and 4.2 A, total xenon flow rates of 5.21 mg/s and 5.74 mg/s, and cathode flow fractions of 10 % and 18 %. The centerline electron density reached a maximum of  $1.8 \times 10^{17} \text{ m}^{-3}$  at the highest cathode flow rate. For all operating conditions, the electron density dropped by a factor of three within  $25^\circ$  of the thruster axis. From Figure 13b it is clear that the electron temperature did not vary greatly with angle from the thruster axis, ranging from 2.0 to 3.5 eV at low cathode flow rates, and from 1.5 to 2.5 eV at the higher cathode flow rates. Note that both operating conditions with a cathode flow of 10% had similar density and temperature profiles, indicating that the change in thruster voltage from 200 V to 250 V did not have a major impact on these characteristics.

The sensitivity of thruster operation to the cathode flow rate is confirmed by the performance measurements reported by Sankovic.<sup>9</sup> In that work it was shown that as the cathode flow rate was increased from 3% to 6% the specific impulse increased from 1450 s to 1620 s, and then it decreased if the cathode flow was increased above 9%. While the physical mechanisms governing the change in specific impulse are not clear, the large changes in electron density and temperature are likely correlated with changes in the plasma conductivity close to the thruster, which will directly impact the accelerating electric field.

#### Ion Current Density

Planar probe measurements 2 m from the thruster at five angles off-axis are shown in Figure 14. These measurements were made at the same thruster operating conditions as were used for the electron density and temperature measurements shown in Figure 12. The ion current density profile is clearly sharply peaked, with the current density dropping by a factor of three within  $22^\circ$  off centerline. A maximum value of  $1.9 \times 10^{-4} \text{ A/cm}^2$  was measured on-axis at a pressure of  $6.7 \times 10^{-4} \text{ Pa}$ . The effect of bleeding in nitrogen to increase the backpressure to  $4 \times 10^{-3} \text{ Pa}$  was to slightly decrease

the ion current density at higher angles and to increase it on centerline, making the distribution more sharply peaked. This result confirms the observations made with the Langmuir probes.

Results obtained using Faraday cups both with and without guard rings are shown in Figure 15. The current density profile obtained from these probes is less sharply peaked, only dropping by a factor of 1.6 within  $22^\circ$  off centerline. As discussed above, the single point measurement obtained using a Faraday cup with a guard ring was substantially lower than that obtained without the guard ring. The effect on the Faraday cups of increasing the tank pressure using nitrogen was similar to that observed using the planar probes, with the current density off-axis decreasing and increasing on-axis.

The consistency of the far-field probe measurements was checked by using the ion current density measurements to estimate the ion density and comparing the result with the Langmuir probe results assuming a singly-ionized quasi-neutral plasma. The ion density was calculated from:

$$n_i = \frac{j_i}{ev_i} \quad (4)$$

where the ion velocity,  $v_i$ , was estimated assuming an accelerating voltage of 300 V. Because the velocity only depends on the square-root of the accelerating voltage errors in this value should not significantly affect this calculation. The result, plotted as a function of ion-current probe-bias voltage, is shown in Figure 16. The shaded region encompasses the error bars on the Langmuir probe result, which reflect the observed fluctuations in that measurement. The agreement between all the probe types is best for ion-current probe bias voltages near -10 V, and the planar probe result is within the Langmuir probe measurement error bars for bias voltages up to -30 V. However, because of the faster sheath growth with the Faraday cups, the densities calculated for those probes reach values up to a factor of two higher than those for the Langmuir and planar probes. The results confirm the importance of guard rings on the ion probes, and suggest that care must be exercised when selecting the ion probe bias voltage.

The impact of the facility conditions on the observed plume characteristics could not be conclusively



identified with the data presented in this paper. With the thruster in the main tank at a pressure of  $6.7 \times 10^{-4}$  Pa, the dominant collision process occurring in the plume was likely resonant charge exchange. For an SPT exhaust velocity of  $1.5 \times 10^4$  m/s the resonant charge exchange cross section is  $\sim 6 \times 10^{-19}$  m<sup>2</sup>,<sup>26,27</sup> yielding a mean free path of  $\sim 10$  m under these conditions. The ion current density measured at a given location is related to that which would be obtained under perfect vacuum by:<sup>19</sup>

$$\frac{j_i}{j_{i,v}} = \exp\left(\frac{-z}{\lambda_{ce}}\right) \quad (5)$$

which shows that resonant charge exchange resulted in a  $\sim 17\%$  decrease in ion current density at 2 m and a  $\sim 33\%$  decrease at 4 m. The angular dependence of these results is not clear given the uncertainty in the ion velocity distribution. However, the charge exchange cross section only increases by a factor of two for an order of magnitude decrease in ion velocity, which suggests that the effects should not be a strong function of angle. Increasing the tank pressure with nitrogen introduced a variety of collisional phenomena to the plume region, including non-resonant charge exchange, momentum transfer, dissociation and ionization of the nitrogen, and could also have perturbed the accelerating field in the thruster region. It was not possible to establish the impact of these processes on the results.

#### Ion Energy

The current measured by the retarding potential analyzer versus the ion suppressor voltage is shown in Figure 17a. The thruster was operated at the design operating condition of 4.5 A and 300 V with a total flow rate of 5.31 mg/s and a cathode flow fraction of 5%. The facility pressure was  $6.7 \times 10^{-4}$  Pa. The noise on the signal was partially attributable to over regulation in the ion suppressor bias power supply. For the data set shown, the electron repeller were biased to a constant -15 V. The slight "knee" in the data trace at approximately 160 V was consistently repeatable in all tests. It was not possible to bias the ion suppressor grid to voltages below 75 V with the system used. This precluded measurement of any low energy charge exchange ions that may have been present. At voltages above 400 V there was a small negative current. This was interpreted as an electron flux caused by incomplete rejection of incident electrons. Possible causes for this

incomplete electron rejection include either too large a distance between the grids or too coarse of grid.

The resulting ion energy distribution is shown in Figure 17b. The oscillations were the manifestation of the noise on the current-voltage characteristic. It was possible to minimize this by applying appropriate signal processing techniques on the raw data, however, no additional information was evident in the signal processed data and, therefore, this additional step was deemed unnecessary. A least-squares Lorentzian curve was fit to the data. This curve had a maximum when the probe was biased to 280 V, indicating that most of the ions had an energy of 280 V relative to the tank ground. This value is close to the discharge voltage of 300 V. A plasma potential of 12 V in the vicinity of the RPA was estimated using Langmuir probe H. Probe H was located directly across the thruster axis at the same distance from the thruster as the RPA as shown in Figure 3. Referencing the RPA result to the plasma potential yields an absolute ion energy of  $\sim 270$  V, indicating that the majority of ions were formed in a region within approximately 30 V of the anode potential. In addition to the dominant ion population at 280 V, there seems to be small secondary peak near 160 V which corresponds to the knee in the current-voltage characteristic. This suggests the presence of a second ionization zone at this potential relative to ground. Although the probe voltage was increased to a maximum of 700 V there was no evidence of doubly charged ions at this location. Note that optical measurements close to the thruster exit plane indicated that up to 20% of the propellant may be doubly ionized,<sup>12</sup> so it is not clear why no doubly ionized xenon ions were detected using the RPA.

Additional scans were taken with electron repeller voltages ranging from -10 V to -30 V in an attempt to assess the impact of the repeller potential on the negative current observed when the ion suppressor was biased above 400 V. For these cases the peak of the V-I characteristic derivative as determined through the least squared error curve fit remained within 2 V of 280 V. However the width of the peak was significantly wider than for those data taken at -10 V. No attempt was made to determine the ion temperature from the width of the experimentally determined ion energy distribution function due to uncertainties in the RPA transmission function. Additional tests are required to examine the variation in ion energy at different positions in the exhaust, verify the cause of the

negative current at higher voltages, and establish the utility of the probe for determining ion temperatures.

### Probe Issues

The use of thin-sheath Langmuir probe theory for the data reduction presumes that the probe radius is always much larger than the Debye length. For the data presented in this paper,  $r_p/\lambda_d$  ranges from a low of two at high angles during the near-field plume measurements to a high of 20 along the centerline at 2-m from the thruster. While other studies have shown that use of thin sheath theory to calculate the electron density across this range yields good agreement with the more detailed calculations of Laframboise,<sup>28</sup> the results could likely be improved both by using Laframboise analysis and by resizing the probes to ensure that the results fall well within either the thin- or thick-sheath regions.

The Debye length also impacts the desired grid spacing on the RPA. To adequately repel all external electrons the grid spacing should be smaller than the Debye length. However, these tests showed that for the conditions near the RPA the 4-mm grid spacing is actually comparable to the Debye length, which may explain the observed electron current at voltages over 400 V. Thus, future RPA designs should be built with smaller grid spacings.

A major concern at the inception of this effort was the possible presence of a non-Maxwellian electron distribution function which would preclude meaningful analysis of the Langmuir probe V-I characteristic. However, while there were many V-I characteristics which might have indicated the presence of a non-Maxwellian distributions, it was not possible to unequivocally eliminate signal noise as the cause of these strange V-I characteristics. In addition, for all operating conditions and probe positions it was always possible to obtain at least a few V-I characteristics which reflected a Maxwellian plasma within  $\sim 8$  V of the plasma potential. Thus, while these results do not eliminate the possibility of a non-Maxwellian electron distribution function, further effort to confirm its existence.

### Conclusions

Preliminary plume characteristics of an SPT-100 thruster were measured at axial distances of 0.3 m, 2 m, and 4-m from the exit plane. Langmuir probes, Faraday cups, planar probes, and a retarding potential analyzer were used to measure the electron density and temperature, ion current density, and ion energy at various angles from the thruster axis. Results showed the centerline electron density decreased from  $\sim 1.8 \times 10^{17} \text{ m}^{-3}$  at 0.3 m to  $2.8 \times 10^{14} \text{ m}^{-3}$  4 m from the thruster, and the temperature stayed between 1.7 eV and 3.5-eV depending on the thruster operating condition. The near-centerline ion current density was  $\sim 1.8 \times 10^4 \text{ A/cm}^2$  2 m from the thruster. The angular density profiles are sharply peaked, with the electron and ion current densities dropping by factors of 2.6 and 3, respectively, within  $22^\circ$  of the thruster axis. A single point ion energy measurement showed that at a distance of 4 m and  $15^\circ$  off-axis the ion energy was approximately 270 V, showing that the ions were likely formed in a region with a potential within 30 V of the anode. The effect of raising the facility pressure from  $6.7 \times 10^{-4} \text{ Pa}$  to  $4 \times 10^{-3} \text{ Pa}$  using nitrogen was to increase the centerline density and decrease the density at high angles, making the plume profile more sharply peaked. Increasing the cathode propellant flow rate from 5% to 9% increased the electron density 0.3 m from the thruster by a factor of three and decreased the electron temperature from 3.5 eV to 2 eV. The measurements also showed that the probe designs could be improved by isolating the Faraday cup wall from the collector and using guard rings on all probes.

### Acknowledgments

The authors would like to thank John Naglowsky, Larry Schultz, Jerry LaPlant, Mike Perez, David Wolford, Peggy Yancer, Gene Pleban, Eli Green, George Jacynycz, Craig Nelson, John Miller, Rob Butler, Gerry Schneider, and Cliff Schroeder for their invaluable assistance during this project.

### References

1. Bober, A.S., et al., "State of Work on Electrical Thrusters in USSR," Proceedings of the 22nd International Electric Propulsion Conference, Viareggio, Italy, Oct. 1991.

2. Belan, N.V., Kim, V.P., Oranskiy, A.I., and Tikhonov, V.B., "Statsionarnyye Plasmennyye Dvigateli," Khar'kovskiy Aviatsionnyy Institut, Khar'kov 1989. (In Russian).
3. Caveny, L.H., Curran, F.M., and Brophy, J.R., "The SDIO Electric Propulsion Program," AIAA Paper 93-1934, June 1993.
4. Kozubsky, K.N, et al., "Plan and Status of the Development and Qualification Program for the Stationary Plasma Thruster," AIAA Paper 93-1787, June 1993.
5. Miller, T. and Bell, R. "An Assessment of the Economic Benefits of SEOTVs for Orbit Transfer," AIAA Paper 93-2218, June 1993
6. Messerole, J., "Launch Costs to GEO Using Solar Powered Orbit Transfer Vehicles," AIAA Paper 93-2219, June 1993.
7. Patterson, M. J., "Low-Isp Derated Ion Thruster Operation," AIAA Paper 92-3203, July 1992; see also NASA TM 105787, August 1992
8. Janson, S.W., "The On-Orbit Role of Electric Propulsion," AIAA Paper 93-2220, June 1993.
9. Sankovic, J.M., Hamley, J.A., and Haag, T.W., "Performance Evaluation of the Russian SPT-100 Thruster at NASA LeRC," IEPC Paper 93-094, Proceedings of the 23rd International Electric Propulsion Conference, Sept. 1993, to be published.
10. Hamley, J. A., Hill, G.M., and Sankovic, J.M., "Power Electronics Development for the SPT-100 Thruster," IEPC Paper 93-044, Proceedings of the 23rd International Electric Propulsion Conference, Sept. 1993, to be published.
11. Pencil, E. J., "Preliminary Results for the Far-Field Plume Sputtering Characterization of the Stationary Plasma Thruster (SPT-100)," IEPC Paper 93-098, Proceedings of the 23rd International Electric Propulsion Conference, Sept. 1993, to be published.
12. Manzella, D.A., "Stationary Plasma Thruster Plume Emissions," IEPC Paper 93-097, Proceedings of the 23rd International Electric Propulsion Conference, Sept. 1993, to be published.
13. Byers, D. C., "Electron Bombardment Thruster Field and Particle Interfaces," Journal of Spacecraft and Rockets, Vol. 16, No. 5, Sept. - Oct. 1979, pp. 289-301.
14. Carruth, M. R., "A Review of Studies on Ion Thruster Beam and Charge-Exchange Plasmas," AIAA Paper 82-1944, Nov. 1982.
15. Carney, L.M., "Evaluation of the Communications Impact of a Low Power Arcjet Thruster," AIAA Paper 88-3105, July 1988.
16. Vaughan, C. and Cassady, J., "An Updated Assessment of Electric Propulsion Technology for Near-Earth Space Missions," AIAA Paper 92-3202, July 1992.
17. Pencil, E.J., et al., "Low Power Arcjet System Spacecraft Impacts," AIAA Paper 93-2392, June 1993.
18. Absalamov, S.K., et al., "Measurement of Plasma Parameters in the Stationary Plasma Thruster (SPT-100) Plume and its Effect on Spacecraft Components," AIAA Paper 92-3156, July 1992.
19. Sovey, J.S. and Patterson, M.J., "Ion Beam Sputtering in Electric Propulsion Facilities," AIAA Paper 2117, June 1991; see also NASA TM 105145.
20. Chung, P. M., Talbot, L., and Touryan, K.J., Electric Probes in Stationary and Flowing Plasmas, Applied Physics and Engineering Vol. II, Springer-Verlag, New York, 1975.
21. Sankovic, J.M. and Jankovsky, R.S., "An Experimental Investigation of the Effective Current Collecting Area of a Spherical Langmuir Probe in an Arcjet Exhaust," AIAA Paper 90-0073, Jan. 1990.
22. Power, J.L., "Ground Correlation Investigation of Thruster/Spacecraft Interactions to be Measured on the IAPS Flight Test," IEPC Paper 84-39, Proceedings of the 17th International Electric Propulsion Conference, Tokyo, Japan, 1984.
23. Wehner, G. and Medicus G., "Reliability of Probe Measurements in Hot Cathode Gas Diodes," Journal of Applied Physics, Vol. 23, No. 9, Sept. 1952, pp. 1035

- 1046.

24. Hershkovitz, N., "How Langmuir Probes Work," in Plasma Diagnostics: Discharge Parameters and Chemistry, Academic Press, Inc., New York, 1989, pp. 113 - 183.

25. Swift, J.D. and Schwar, M.J., Electric Probes for Plasma Diagnostics, American Elsevier Publishing Co., New York, 1970.

26. Rapp, D. and Francis, W.E., "Charge Exchange between Gaseous Ions and Atoms," Journal of Chemical Physics, Vol. 37, No. 11, Dec. 1962, pp 2631 - 2645.

27. Smirnov, B.M. and Chibisov, M.I., "Resonance Charge Transfer in Inert Gases," Soviet Physics - Technical Physics, Vol. 10, No. 1, July 1965, pp 88 - 92.

28. Salhi, A., Myers, R.M., and Turchi, P.J., "Experimental Investigation of a Hollow Cathode Discharge," IEPC Paper 93-025, Proceedings of the 23rd International Electric Propulsion Conference, Sept. 1993, to be published.

Table I - Probe types and positions used to characterize far-field SPT-100 plume.

Probe designation	Probe type	Distance from thruster, m	Angle off-axis, degrees
A	Spherical Langmuir	2	7.5
B	Spherical Langmuir	2	37.5
C	Spherical Langmuir	2	52.5
D	Spherical Langmuir	2	67.5
E	Spherical Langmuir	2	82.5
F	Spherical Langmuir	2	-37.5
G	Spherical Langmuir	4	0
H	Spherical Langmuir	4	15
I	Planar	2	0
J	Planar	2	22.5
K	Planar	2	37.5
L	Planar	2	52.5
M	Planar	2	-22.5
N	Faraday cup	2	0
O	Faraday cup	2	22.5
P	Faraday cup	2	37.5
Q	Faraday cup	2	52.5
R	Faraday cup w/Guard Ring	2	37.5
S	Retarding Potential Analyzer	4	15

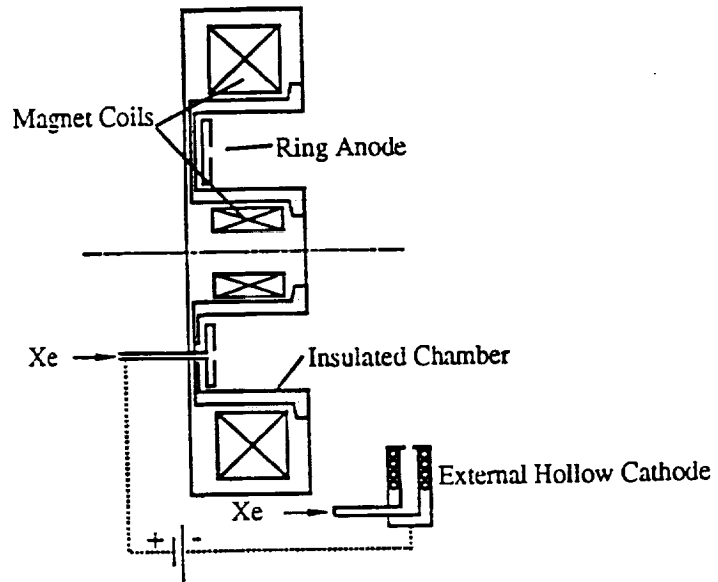


Figure 1: Schematic of the SPT

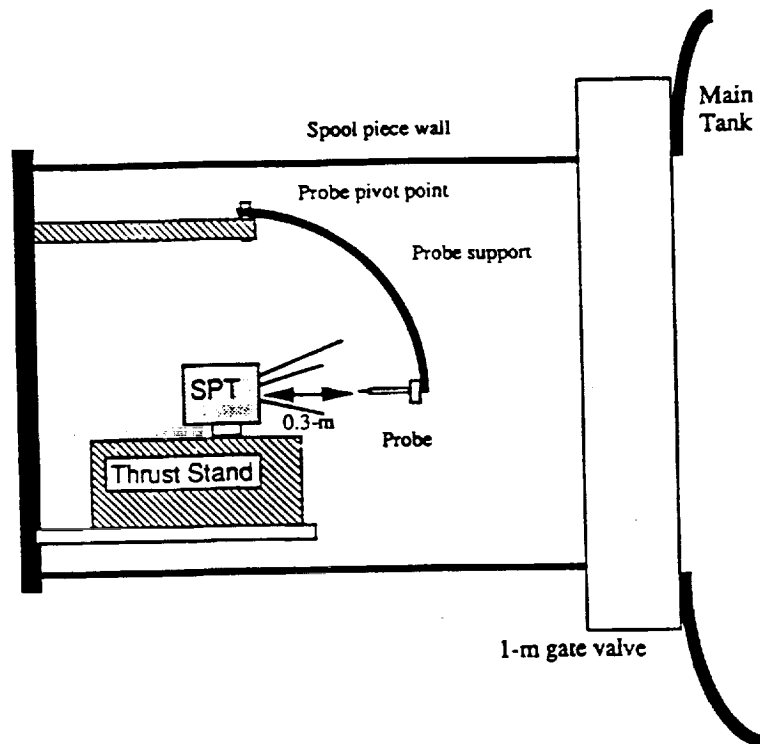


Figure 2 - Near-field SPT-100 Langmuir probe arrangement.

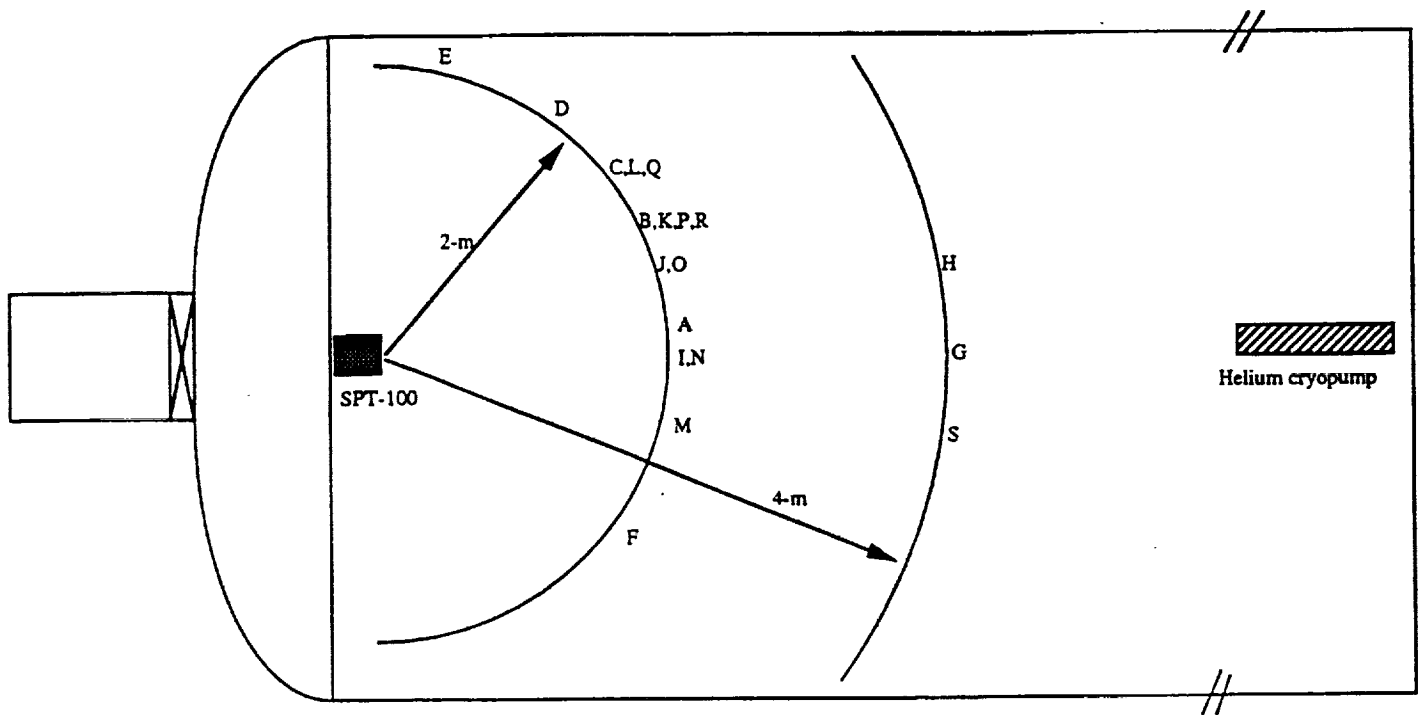


Figure 3 - Far-field probe arrangement. Letters correspond to individual probes listed in Table 1 and show approximate relative positions.

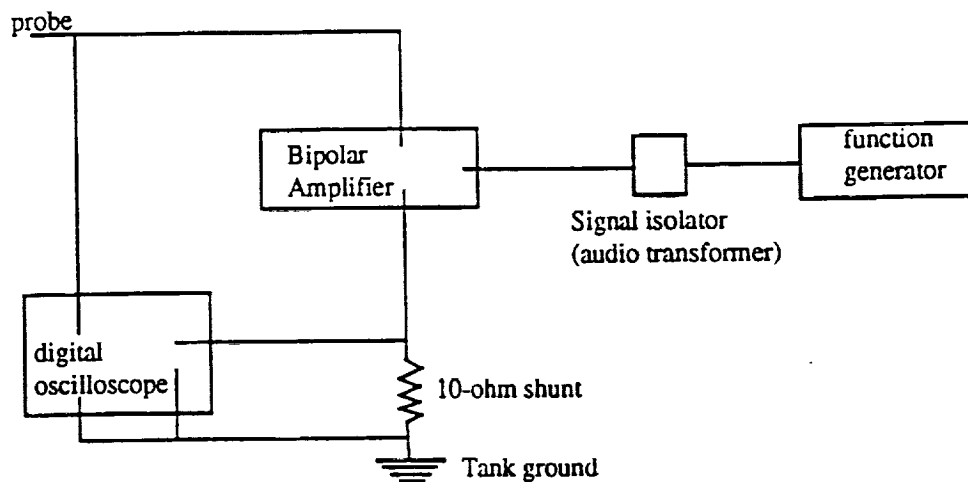


Figure 4 - Circuit used to bias Langmuir probes

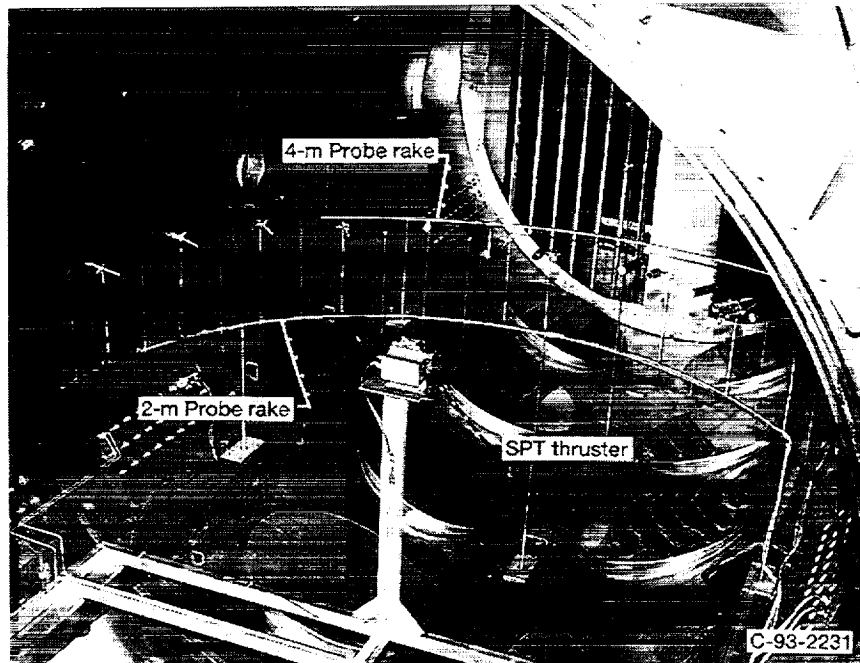


Figure 5 - Photograph showing SPT thruster and probe arrangement used for the far-field plume studies in Tank 5 at NASA LeRC.

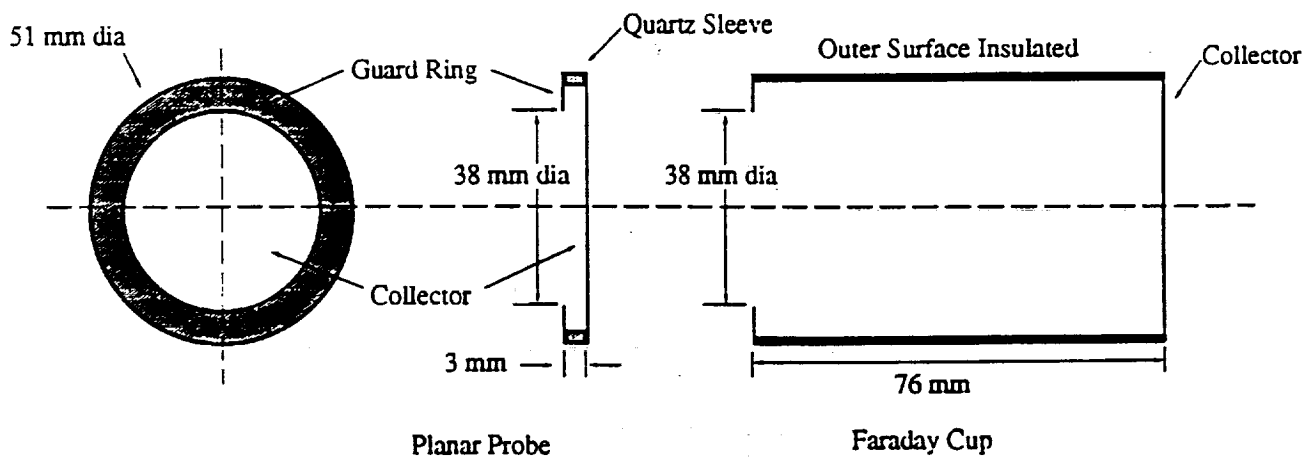


Figure 6 - Schematic of Planar Probe and Faraday Cup

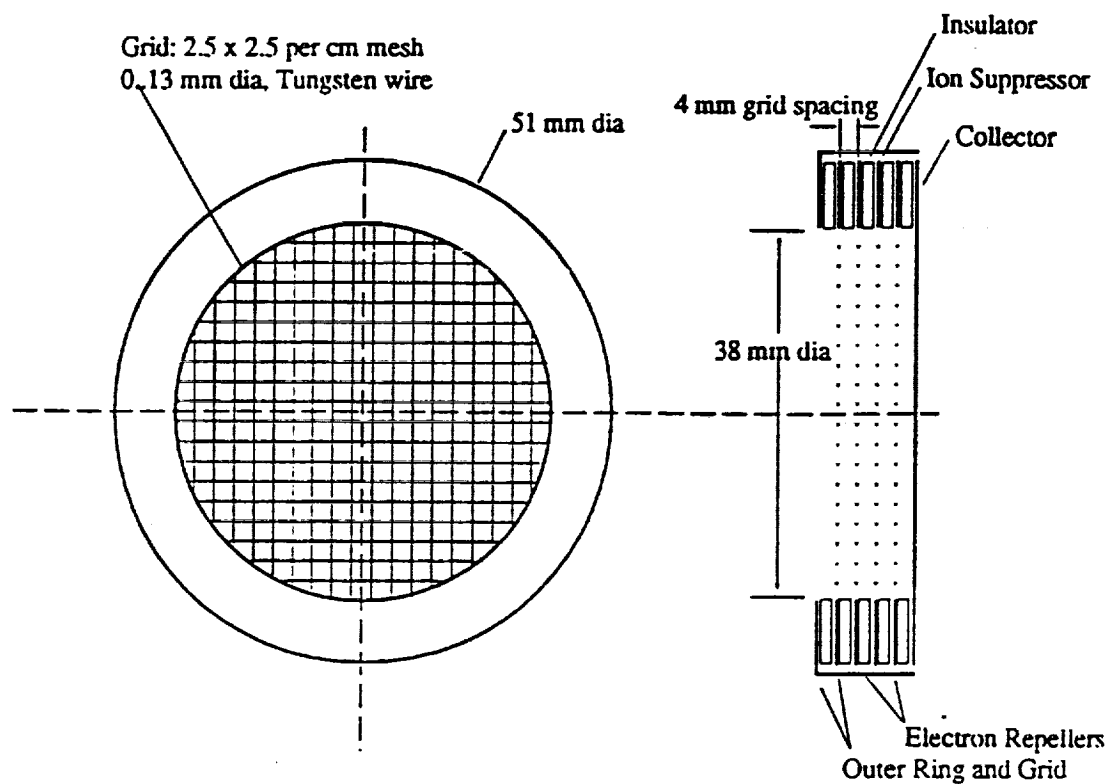


Figure 7 - Schematic of Retarding Potential Analyzer (RPA)

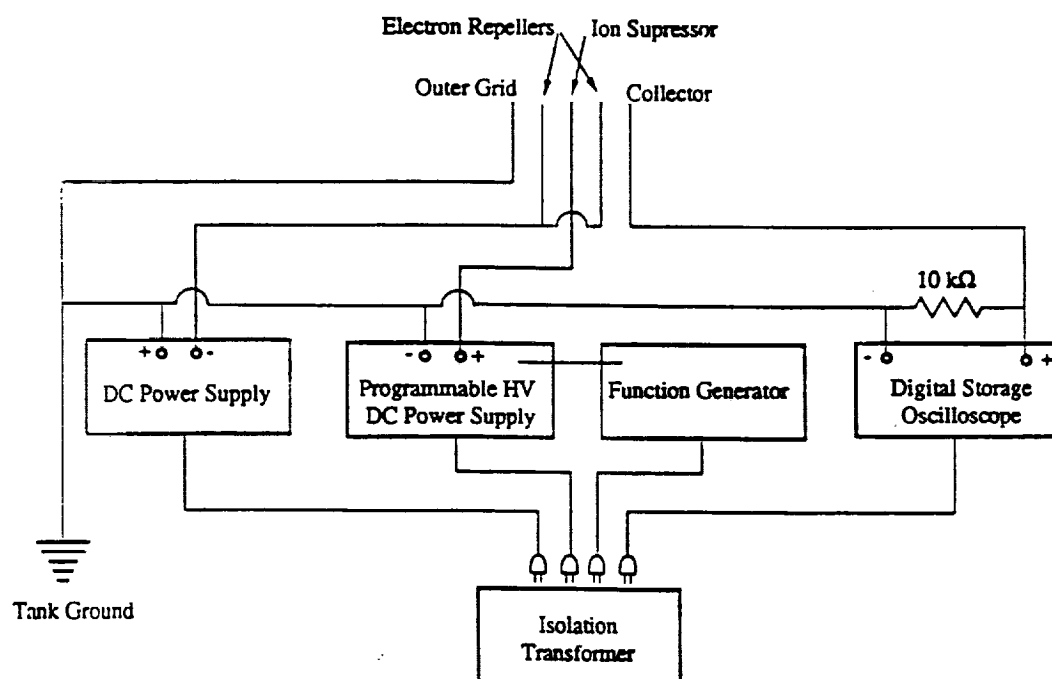


Figure 8 - RPA Circuit Schematic



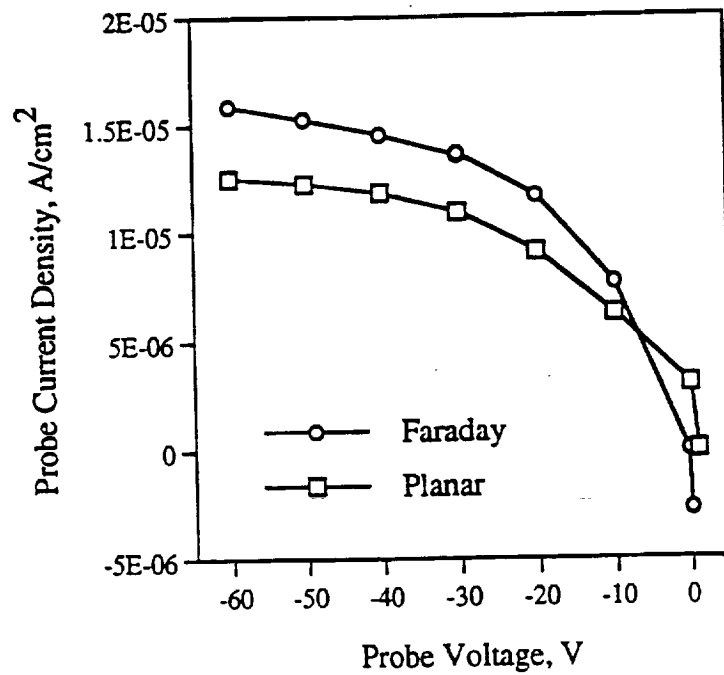


Figure 9 - Faraday cup and planar probe comparison 2 m from thruster, 52.5 degrees off centerline. Facility pressure of  $6.7 \times 10^{-4}$  Pa.

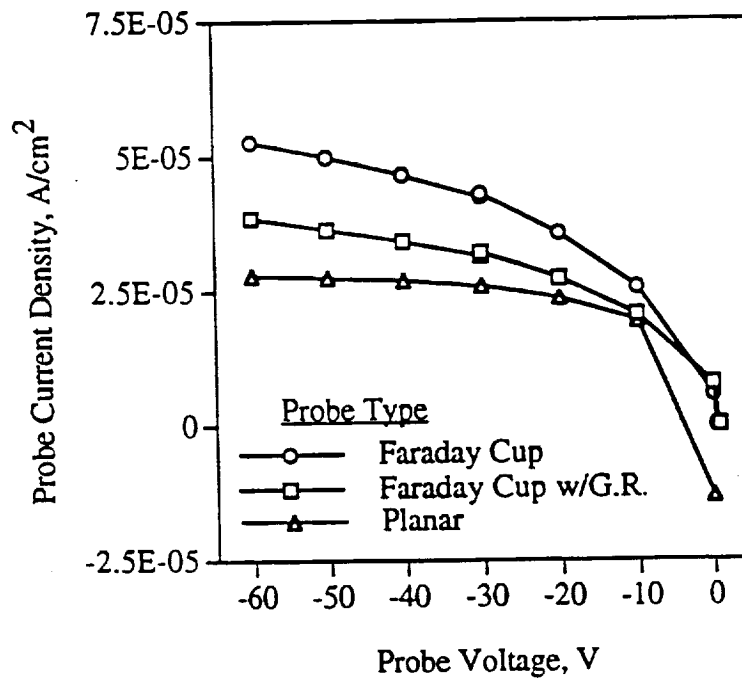


Figure 10 - Faraday cup, Faraday with a guard ring, and planar probe comparison. 2 m from thruster, 37.5 degrees from centerline.

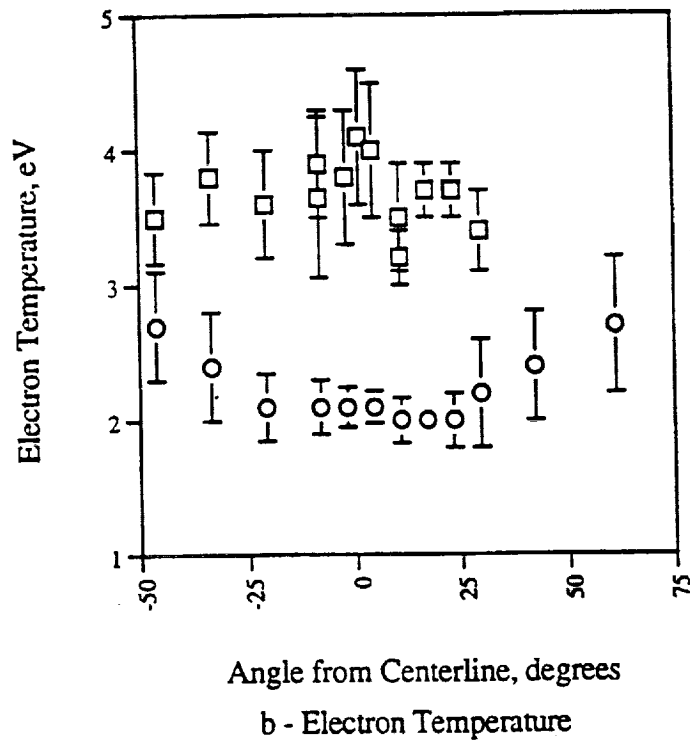
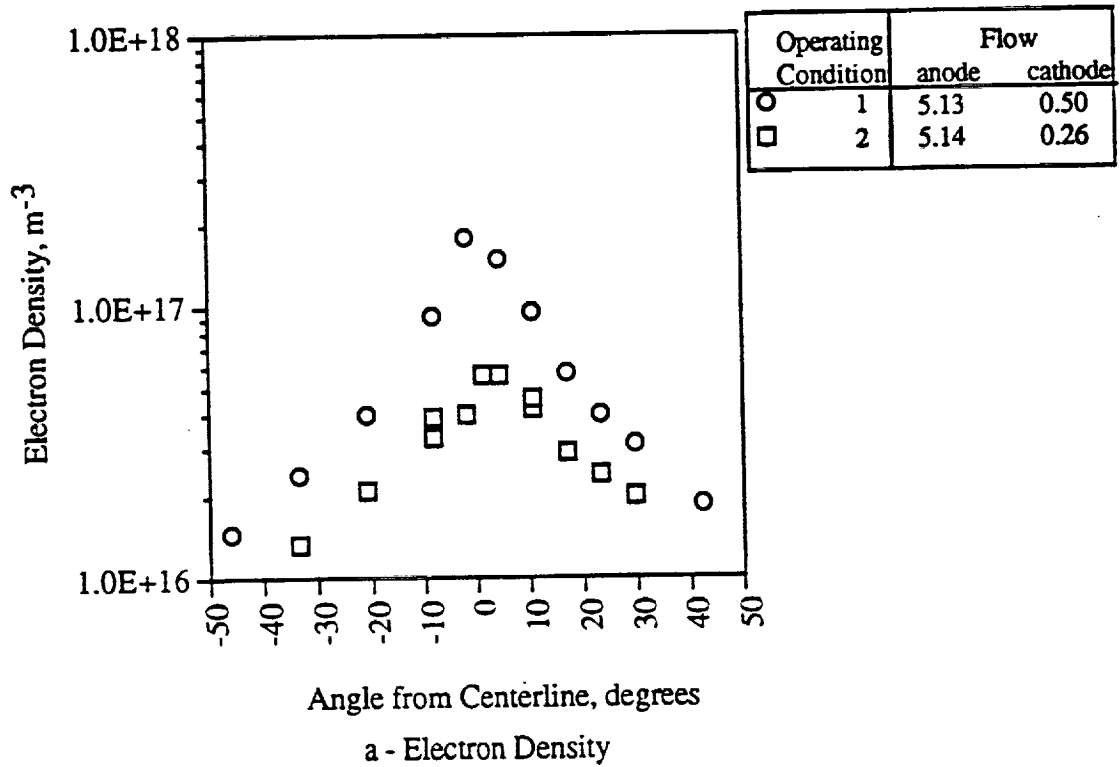
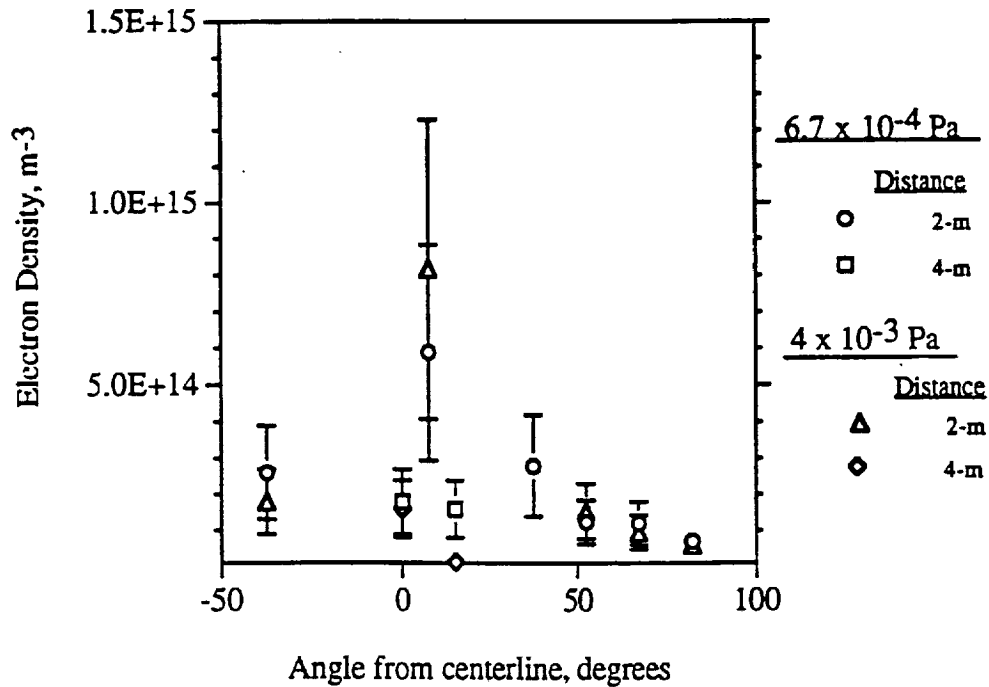
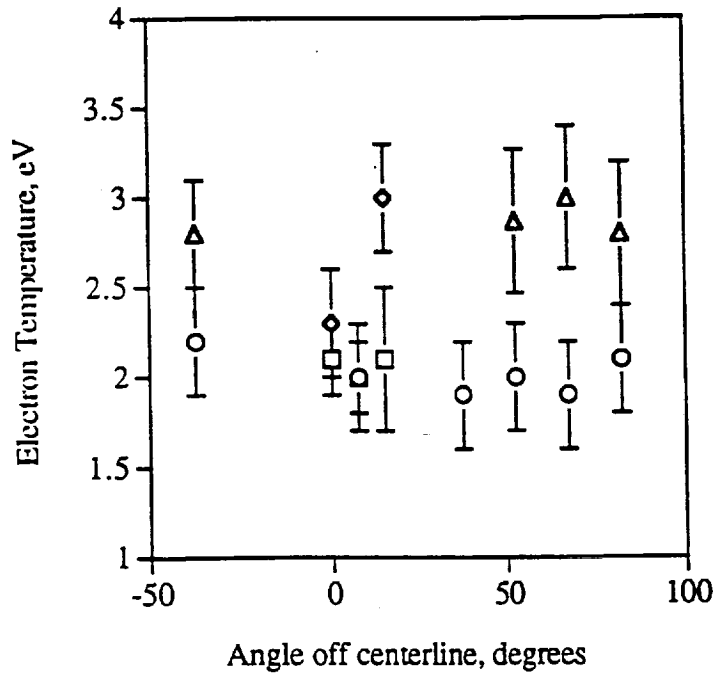


Figure 11 - Electron density and temperature 0.31 m from the SPT as a function of angle off-axis. Thruster voltage and current of 300 V and 4.5 A, respectively, and two flow rates.



a - Electron density

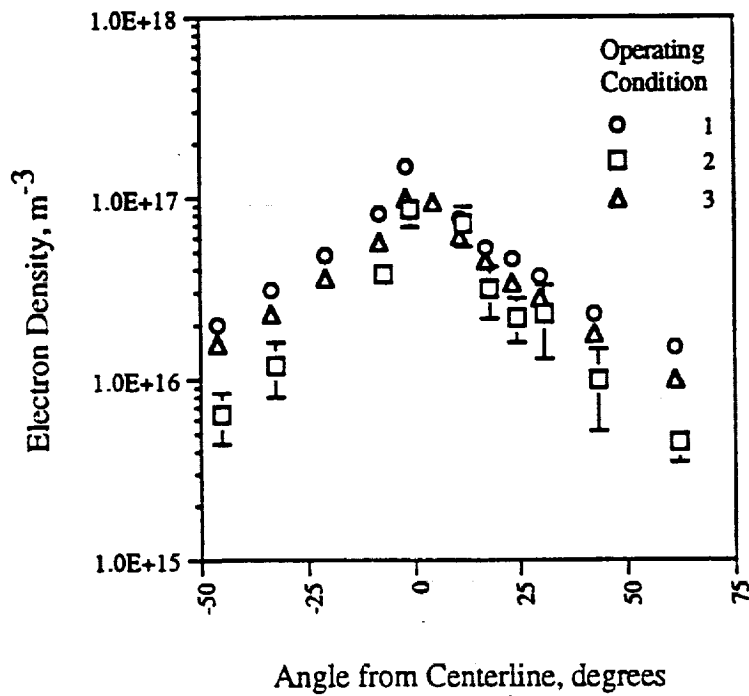


b - Electron Temperature

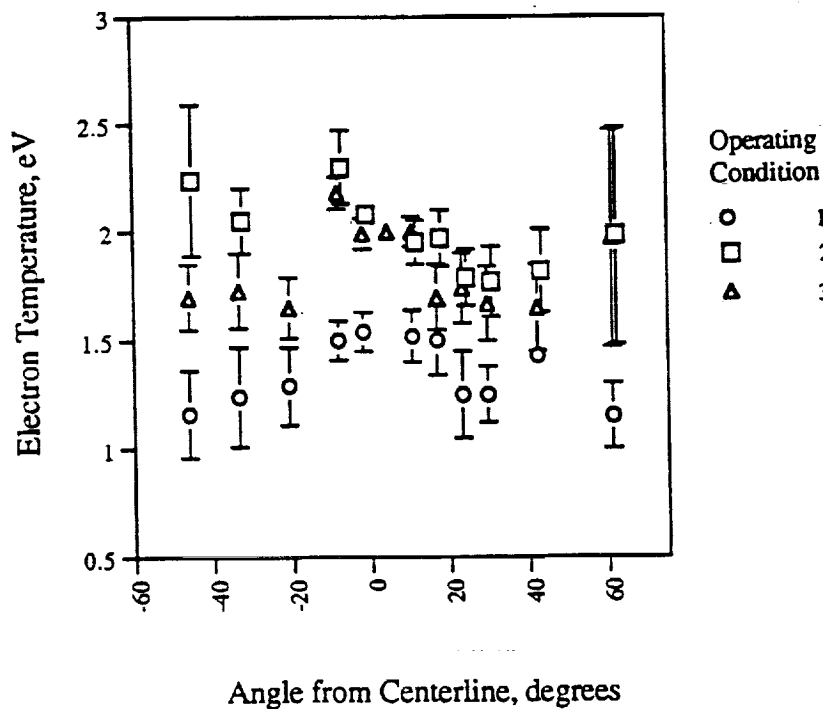
Figure 12 - Far-field electron density and temperature at 2 m and 4 m as a function of angle off centerline for two tank pressures. Thruster operating conditions:

(1)  $6.7 \times 10^{-4} \text{ Pa}$ : Anode flow: 5.05 mg/s, cathode flow: 0.26 mg/s, V: 300 V, I: 4.5 A.

(2)  $4 \times 10^{-3} \text{ Pa}$ : Anode flow: 4.85 mg/s, cathode flow: 0.21 mg/s, V: 300 V, I: 4.5 A.



a - Electron density



b - Electron Temperature

Figure 13 - Electron density and temperature 0.31-m from thruster vs. angle from thruster axis for 3 SPT thruster operating conditions:

- (1) Anode flow: 4.7-mg/s, cathode flow: 1.03-mg/s, V: 200-V, I: 4.23-A;
- (2) Anode flow: 4.71-mg/s, cathode flow: 0.5-mg/s, V: 250-V, I: 4.07-A;
- (3) Anode flow: 4.71-mg/s, cathode flow: 0.5-mg/s, V: 200-V, I: 4.12-A.

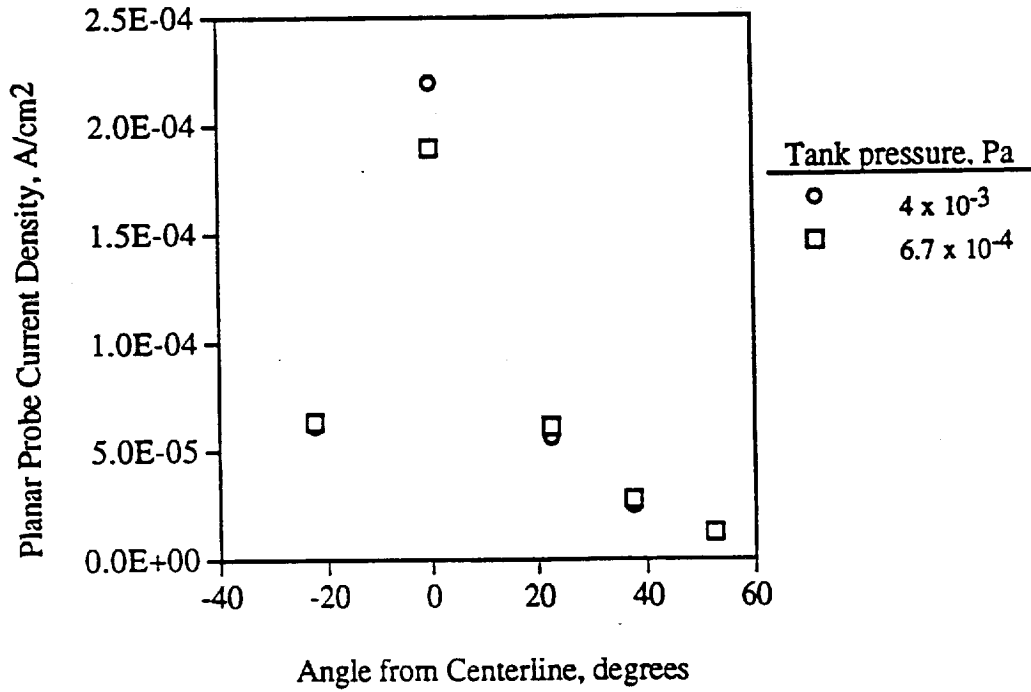


Figure 14 - Planar probe ion current densities 2 m from the thruster for two tank pressures. Nitrogen was used to raise the tank pressure.

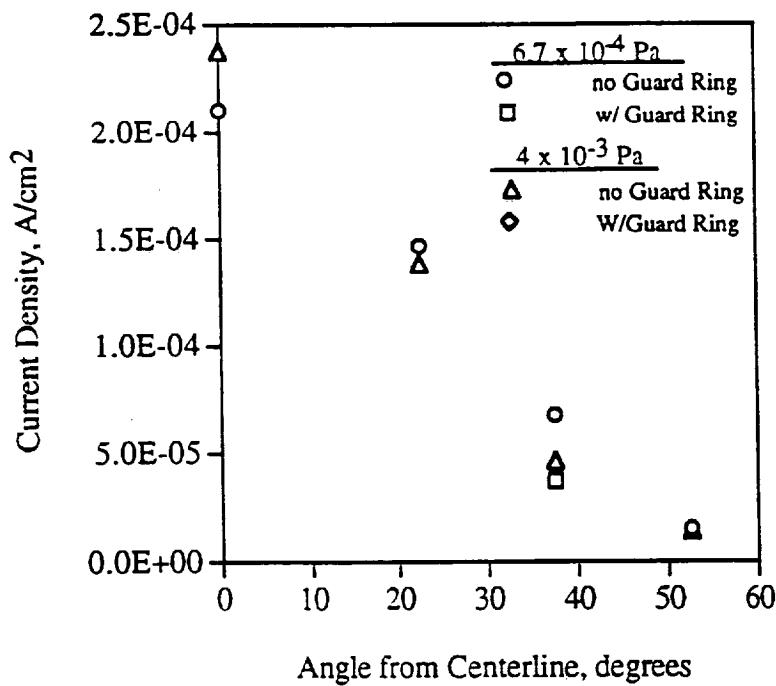


Figure 15 - Faraday probe measurements 2 m from the thruster as a function of angle from centerline for two tank pressures. Probes without and with guard rings are shown.

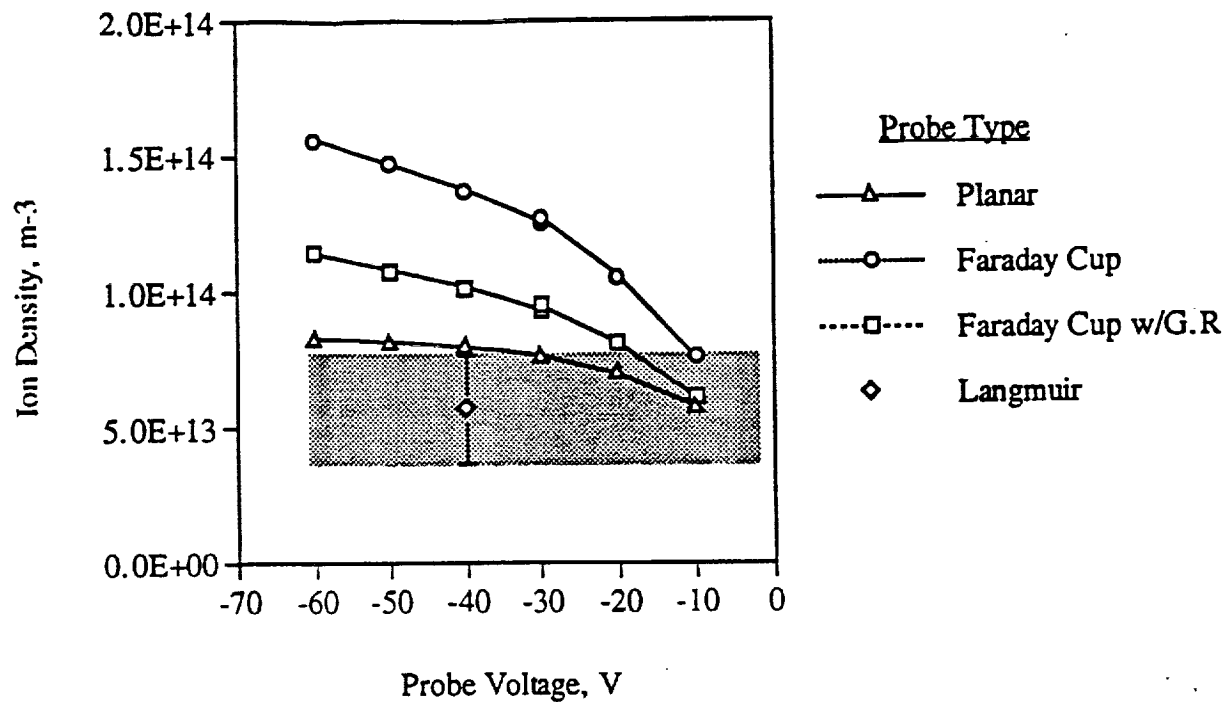


Figure 16 - Calculated ion density as a function of probe type and probe voltage. Acceleration voltage of 300 V assumed, 2 m from thruster, 37.5 deg. from centerline.

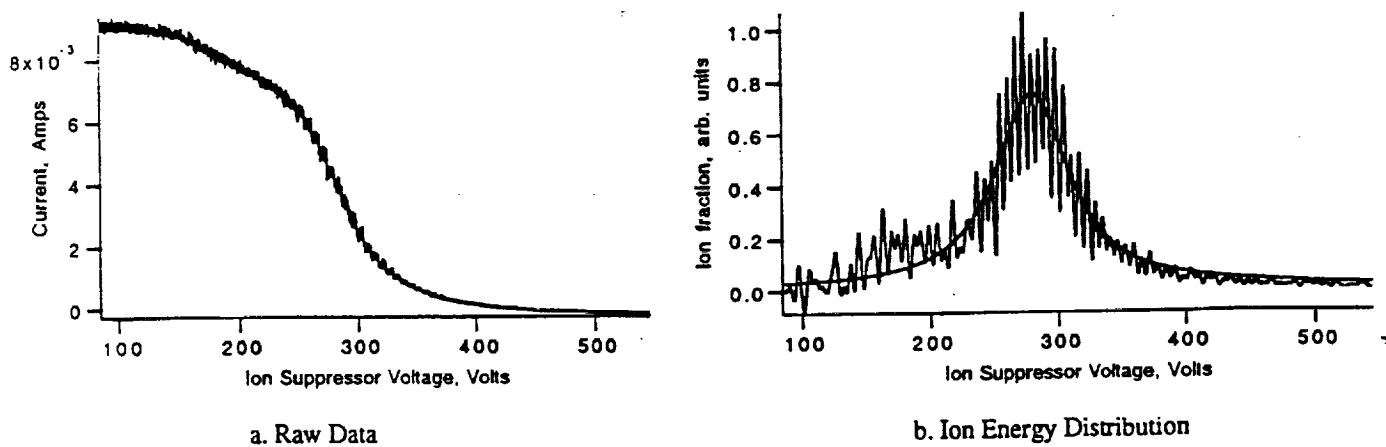


Figure 17 - RPA Results for Probe 4m from Thruster, -15° off-axis. Facility Pressure  $6.7 \times 10^{-4}$  Pa.



REPORT DOCUMENTATION PAGE			Form Approved OMB No. 0704-0188	
Public reporting burden for this collection of information is estimated to average 1 hour per response, including the time for reviewing instructions, searching existing data sources, gathering and maintaining the data needed, and completing and reviewing the collection of information. Send comments regarding this burden estimate or any other aspect of this collection of information, including suggestions for reducing this burden, to Washington Headquarters Services, Directorate for Information Operations and Reports, 1215 Jefferson Davis Highway, Suite 1204, Arlington, VA 22202-4302, and to the Office of Management and Budget, Paperwork Reduction Project (0704-0188), Washington, DC 20503.				
1. AGENCY USE ONLY (Leave blank)	2. REPORT DATE February 1994	3. REPORT TYPE AND DATES COVERED Final Contractor Report		
4. TITLE AND SUBTITLE  Stationary Plasma Thruster Plume Characteristics		5. FUNDING NUMBERS  WU-506-42-31 C-NAS3-25266		
6. AUTHOR(S)  Roger M. Myers and David H. Manzella				
7. PERFORMING ORGANIZATION NAME(S) AND ADDRESS(ES)  Sverdrup Technology, Inc. Lewis Research Center Group 2001 Aerospace Parkway Brook Park, Ohio 44142		8. PERFORMING ORGANIZATION REPORT NUMBER  E-8406		
9. SPONSORING/MONITORING AGENCY NAME(S) AND ADDRESS(ES)  National Aeronautics and Space Administration Lewis Research Center Cleveland, Ohio 44135-3191		10. SPONSORING/MONITORING AGENCY REPORT NUMBER  NASA CR-194454		
11. SUPPLEMENTARY NOTES Prepared for the 23rd International Electric Propulsion Conference sponsored by the American Institute of Aeronautics and Astronautics, Seattle, Washington, September 13-16, 1993. Project Manager, James S. Sovey, Space Propulsion Technology Division, organization code 5330, NASA Lewis Research Center, (216) 433-7454.				
12a. DISTRIBUTION/AVAILABILITY STATEMENT  Unclassified - Unlimited Subject Categories 20 and 75		12b. DISTRIBUTION CODE		
13. ABSTRACT (Maximum 200 words)  Stationary Plasma Thrusters (SPTs) are being investigated for application to a variety of near-term missions. This paper presents the results of a preliminary study of the thruster plume characteristics which are needed to assess spacecraft integration requirements. Langmuir probes, planar probes, Faraday cups, and a retarding potential analyzer were used to measure plume properties. For the design operating voltage of 300 V the centerline electron density was found to decrease from $\sim 1.8 \times 10^{17} \text{ m}^{-3}$ at a distance of 0.3 m to $1.8 \times 10^{14} \text{ m}^{-3}$ at a distance of 4 m from the thruster. The electron temperature over the same region was between 1.7 and 3.5 eV. Ion current density measurements showed that the plume was sharply peaked, dripping by a factor of 2.6 within 22 degrees of centerline. The ion energy 4 m from the thruster and $15^\circ$ off-centerline was $\sim 270$ V. The thruster cathode flow rate and facility pressure were found to strongly affect the plume properties. In addition to the plume measurements the data from the various probe types were used to assess the impact of probe design criteria.				
14. SUBJECT TERMS  Electric propulsion; Plasma dynamics		15. NUMBER OF PAGES 22		
		16. PRICE CODE A03		
17. SECURITY CLASSIFICATION OF REPORT Unclassified	18. SECURITY CLASSIFICATION OF THIS PAGE Unclassified	19. SECURITY CLASSIFICATION OF ABSTRACT Unclassified	20. LIMITATION OF ABSTRACT	